

Highlights

Reducing RES Droughts through the integration of wind and PV

Boris Morin, Aina Maimo Far, Damian Flynn, Conor Sweeney

- Energy droughts are defined as periods of low production
- Three models compared to evaluate renewable energy droughts in Ireland
- Analysis of 45 years of ERA5 weather data for energy drought trends
- Diverse energy mix reduces drought frequency and duration significantly
- Model choice impacts energy drought results

Reducing RES Droughts through the integration of wind and PV

Boris Morin^a, Aina Maimo Far^a, Damian Flynn^b, Conor Sweeney^a

^a*University College Dublin, School of Mathematics and Statistics, , Dublin, , Ireland*

^b*University College Dublin, School of Electrical and Electronic Engineering, , Dublin, , Ireland*

Abstract

The dependence of renewable energy sources (RES) such as wind and photovoltaic (PV) systems on the weather poses a critical challenge for energy systems. This study investigates the impact of targeting a balanced distribution of wind and PV capacity on reducing periods of low renewable generation, known as RES droughts. Three different RES models are used to estimate the capacity factors for different installed capacities of wind and PV energy. The skill of the RES models is quantified by comparing capacity factor time series to observed data. Their skill at representing RES droughts is also quantified. The RES models are used to generate a 45-year hourly time series of RES generation, enabling analysis of the frequency, duration and return periods of RES droughts at a climatological scale. Results show the importance of using an accurate, validated RES model for RES drought risk assessment. The addition of PV capacity to a wind-dominated system results in a large reduction in the frequency and duration of RES droughts, as well as reducing seasonal drought patterns. These findings underscore the importance of diversification in RES capacity to enhance energy security and resilience.

Keywords: RES Drought, Wind Power, Solar PV Power, Renewable Energy Sources, Return Periods

1. Introduction

The EU aims to generate at least 69% of its electricity from renewable energy sources (RES) by 2030, up from 41% in 2022 (EuroStat, 2023). While

4 this transition is essential for reducing greenhouse gas emissions, it also high-
5 lights the challenge of managing the variability of weather-dependent en-
6 ergy sources such as wind and photovoltaic (PV) power. This challenge is
7 compounded by the increasing electrification of energy sectors, which places
8 greater demand on the power system and makes it more sensitive to meteo-
9 rological conditions (Bloomfield et al., 2021, 2016; van der Wiel et al., 2019).
10 Periods of low renewable generation, known as *Dunkelflaute* or RES droughts,
11 pose significant risks to system adequacy and energy security, emphasizing
12 the need for a resilient energy system to meet both growing electricity de-
13 mand and decarbonization targets.

14 This study focuses on Ireland, a region with a strong reliance on wind
15 power, which has ambitious targets for PV power expansion. This case study
16 provides valuable insights into the potential benefits of diversifying the re-
17 newable energy mix on RES droughts. The performance of different RES
18 models are compared, and a 45-year time series of RES generation is pro-
19 duced. The results highlight the role of increased PV capacity in reducing
20 RES drought risks, offering insights for policymakers and energy planners.

21 For this study, a RES drought event is defined as occurring when the
22 average capacity factor (CF) remains below a fixed threshold for a given
23 duration, following the methodology used in other research (Kaspar et al.,
24 2019; Ohba et al., 2022; Mockert et al., 2023; Mayer et al., 2023). Alterna-
25 tive methods exist for defining RES droughts. One approach uses relative
26 CF thresholds that change over the year to account for seasonal variations
27 in renewable energy generation (Raynaud et al., 2018; Rinaldi et al., 2021;
28 Gangopadhyay et al., 2022; Allen and Otero, 2023; Kapica et al., 2024). An-
29 other common method relies on percentile-based thresholds, where drought
30 events are defined by identifying periods of unusually low generation relative
31 to historical production levels, typically based on the lowest production per-
32 centiles (Bracken et al., 2024; Allen and Otero, 2023). Additionally, some
33 studies combine these definitions with metrics that incorporate the demand
34 side of energy consumption, analysing the balance between supply and de-
35 mand during drought periods (Raynaud et al., 2018; Rinaldi et al., 2021;
36 Allen and Otero, 2023; Bracken et al., 2024). In this paper, the focus is
37 exclusively on energy generation, and a fixed threshold approach to define
38 RES droughts is used, which facilitates consistent inter-comparison between
39 scenarios with different installed wind and PV capacities.

40 RES droughts are identified using onshore wind and PV CF time series. In
41 this study, three different datasets are used, all of which are driven by ERA5

data (Hersbach et al., 2020). Two of the datasets are part of C3S Energy (C3S-E) (, C3S), an energy-based operational dataset produced by the EU Copernicus Climate Change Service Dubus et al. (2023). One of the C3S-E datasets provides CF time series aggregated at the national scale, while the other provides the CF time series at each grid point, at the ERA5 resolution of 0.25° . The third dataset was generated using the Atlite model Hofmann et al. (2021), which converts the ERA5 atmospheric data to a generation time series using specified wind turbine and PV panel models. Atlite is an open-source tool developed by PyPSA Hofmann et al. (2021) and is widely used for estimating wind and PV generation Mockert et al. (2023); Li et al. (2023); Parzen et al. (2023); Ali Khan Niazi and Victoria (2023).

The datasets used in this study are detailed in section 2, which describes their characteristics and relevance for evaluating RES droughts. Section 3 outlines the RES models used to simulate wind and PV generation and provides the methodology for defining and identifying RES drought events, including the thresholds and metrics applied. In section 4, the models are first verified against observed energy data to assess their accuracy, followed by an analysis of RES drought occurrences for two scenarios with different ratios of installed wind to PV capacities. Finally, section 5 offers a discussion of the results in the context of energy reliability and future planning, followed by the main conclusions and recommendations for further research.

2. Data

This study uses publicly available datasets to construct and validate the models for estimating the CF of wind and PV energy. The primary data sources include: EirGrid and SONI, the transmission system operators (TSO) for the Republic of Ireland and Northern Ireland, respectively; the ERA5 reanalysis dataset; and the C3S-E datasets.

2.1. Wind and PV Capacity Factor

EirGrid, the TSO for the Republic of Ireland, and SONI, the Northern Ireland TSO, provide detailed datasets on all wind and PV farms across the island of Ireland (Republic of Ireland and Northern Ireland) from 1990 to the present SONI. These datasets include information such as each farm’s installed capacity, name, and connection date. To enhance the accuracy of this data, the longitude and latitude for each farm were manually determined

through online searches. For simplicity, this data will be referred to as originating from EirGrid, as all-island data was directly obtained from EirGrid, and the combined regions of the Republic of Ireland and Northern Ireland will be referred to as Ireland throughout the remainder of this document.

The spreadsheet available from the EirGrid website contains two key variables: generation and availability. Generation is the energy that a RES farm actually contributed to the grid, which may include limitations introduced by the TSO to maintain grid stability, such as constraints and curtailment. Availability represents the energy that would have been generated from a RES farm if no grid constraints had been applied, making it representative of the weather-related response. Generation and availability values are available from 2014 onward for wind power and from 2018 onward for PV power, although PV availability data only became present in the Republic of Ireland in 2023. This study focuses on availability for all analyses.

2.2. Atmospheric Variables

Atlite and C3S-E datasets are driven by the ERA5 reanalysis Hersbach et al. (2020), produced by the European Centre for Medium-Range Weather Forecasts (ECMWF). This global gridded dataset provides hourly atmospheric variables from 1940 to the present at a horizontal resolution of 0.25° . It is widely used for estimating PV and wind energy Mockert et al. (2023); Dubus et al. (2023); Brown et al. (2021); Otero et al. (2022). Table 1 lists the ERA5 variables used by Atlite and C3S-Energy.

Table 1: ERA5 variables used to calculate wind and PV generation

ERA5 name	variable
100 metre zonal and meridional wind speed	u_{100}, v_{100}
2 metre temperature	$t2m$
Surface net solar radiation	ssr
Surface solar radiation downwards	$ssrd$
Top of atmosphere incident radiation	$tisr$
Total sky direct solar radiation at surface	$fdir$

2.3. C3S Energy

The EU Copernicus Climate Change Service developed the C3S-E renewable energy dataset for Europe Dubus et al. (2023), using ERA5 atmospheric

101 variables and weather-to-energy models. This dataset provides hourly CF for
 102 wind and PV energy from 1979 to the present. The data are available on the
 103 same grid as the ERA5 data, which has a horizontal resolution of 0.25° . The
 104 time series are also available for download at two aggregated scales: regional
 105 (NUTS 2) and national.

106 The C3S-E dataset estimates wind energy using wind speeds at 100 me-
 107 tres (u_{100} , v_{100}) and a standard turbine model, the Vestas V136/3450, with
 108 a fixed hub height of 100 meters. This choice is based on expert advice and
 109 the trend in wind turbine installation. The PV generation model used by
 110 C3S-E uses two ERA5 variables: surface solar radiation downwards (*ssrd*)
 111 and air temperature (*t2m*). PV generation is calculated multiple times, us-
 112 ing the same model with different azimuth and tilt angles. The results are
 113 aggregated based on a statistical distribution of the module angles based on
 114 the geographical location Saint-Drenan et al. (2018).

115 3. Methods

116 This study uses three datasets to analyse RES droughts across the island
 117 of Ireland. Data downloaded from C3S-E were used to obtain two datasets:
 118 one based on national-level data (C3S-E N), and another on grid-level data
 119 (C3S-E G). The third dataset was computed using the Atlite model (Atlite).

120 3.1. C3S-Energy National

121 For national-level analyses, the aggregated CF time series provided by
 122 C3S-E were used at two levels: Republic of Ireland (NUTS0: IE) and North-
 123 ern Ireland (NUTS2: UKN0). These are based on the assumption by C3S-E
 124 that RES generation occurs at every ERA5 grid point in Ireland. We com-
 125 puted a weighted average of these, based on the installed capacity of each
 126 one, to represent the total CF for Ireland.

127 3.2. C3S-E Gridded

128 The gridded dataset from C3S-E was used to create CF datasets which
 129 account for the location of RES farms in Ireland. A list of the RES farms in
 130 Ireland was compiled, including each farm’s latitude, longitude and installed
 131 capacity. Using these coordinates, the nearest grid point on the C3S-E grid
 132 was identified for each farm. The CF values from the C3S-E dataset corre-
 133 sponding to these grid points were retrieved. A weighted average of the CF
 134 values was calculated, with the installed capacity of each farm serving as the

weight, to construct the CF time series for Ireland. This process resulted in a time series of RES generation for each energy source (wind and PV) for Ireland, which takes the location of the RES farms into account.

3.3. Atlite

Atlite transforms weather data into energy data using the gridded ERA5 data and the locations of existing RES farms, as described in C3S-E G. ERA5 data for wind speed at 100 metres (u_{100} , v_{100}) are used to calculate wind generation, while the ERA5 radiation variables (ssr , $ssrd$, $tisr$, and $fdir$) and air temperature ($t2m$) are used to calculate PV generation. A key distinction between C3S-E and Atlite lies in their representation of wind turbines and PV panels. This study identifies the most appropriate wind turbine power curve to use from the 121 power curves made available by Renewables.ninja Staffell and Pfenninger (2016). The selection of a specific wind turbine and PV panel characteristics is further discussed and explained in section 4.1.

3.4. Energy Scenarios

In addition to analysing wind and PV generation separately, a combined CF was computed for each model by averaging wind and PV generation, weighted by their installed capacities at the end of 2023 (5.9 GW for wind power and 0.6 GW for PV power). This configuration is referred to as the 91W-9PV scenario, reflecting the distribution of 91% wind and 9% PV capacity. Given that PV capacity in Ireland is low in 2023, and to explore how a more balanced distribution of wind and PV capacities might impact RES droughts, this study also considered a second scenario, referred to as 57W-43PV, where the installed PV capacity is assumed to increase to 8.6 GW, while wind capacity rises to 11.45 GW. These values are based on targets outlined in the roadmap published by the 2024 Climate Action Plan of Ireland (2023). This study does not include offshore wind in the analysis. Recent reports suggest that even by 2030, Ireland is unlikely to have any significant new offshore wind farms, with projected offshore capacity expected to remain near zero using realistic scenarios Ireland (2024).

New time series were generated for both the Atlite and C3S-E G PV models, incorporating a revised distribution of installed capacity across Ireland as specified in the roadmap. For wind power, the CF time series remains unchanged, as significant shifts in the location of wind farms are not expected. In total, twelve CF time series were analysed in this study, six for individual

171 wind and PV CF (three models for each source) in the 91W-9PV scenario,
172 and an additional six time series that include the combined CF for 91W-9PV
173 and 57W-43PV scenarios across the different models.

174 It is important to note that the specific capacity values used in this study
175 are illustrative and are not intended to reflect precise future realities. Instead,
176 they serve to explore the impact of transitioning from a wind-dominated sys-
177 tem (91W-9PV) to a more evenly distributed system (57W-43PV). This ap-
178 proach allows for a comparative analysis between the two scenarios, assessing
179 how the balance of RES capacity affects the occurrence of RES droughts.

180 3.5. *RES Drought Definition*

181 In this study, a RES drought event was defined as occurring when the 24-
182 hour moving average of CF remains below a fixed threshold of 0.1 for a period
183 of longer than 24 hours. The choice of this threshold is somewhat arbitrary,
184 but aligns with similar studies on low renewable energy production Kaspar
185 et al. (2019); Ohba et al. (2022); Mayer et al. (2023). By using a 24-hour
186 moving average, fewer but longer-lasting events were captured compared to
187 using the raw CF time series, which can be more sensitive to short-term
188 fluctuations. A fixed threshold approach was chosen in this study to enable
189 consistent inter-comparison between datasets.

190 The moving average approach smooths out short-term fluctuations, so
191 that brief periods above the threshold do not interrupt an otherwise con-
192 tinuous low-CF period (Fig. 1). This means that a single hour above the
193 threshold does not "break" a drought event if it is surrounded by prolonged
194 low-generation hours. As a result, fewer but longer-lasting drought events
195 are identified, which may better reflect real-world conditions where energy
196 supply constraints persist over extended periods.

197 4. Results

198 4.1. *Verification*

199 The accuracy of the datasets used in this study was verified, before con-
200 tinuing to the analysis of RES droughts. For the verification process, time-
201 varying values of installed capacity were used to account for changes in RES
202 development over the verification period. This step allowed us to assess how
203 well the datasets represent the production of renewable energy by comparing
204 them against observed data.

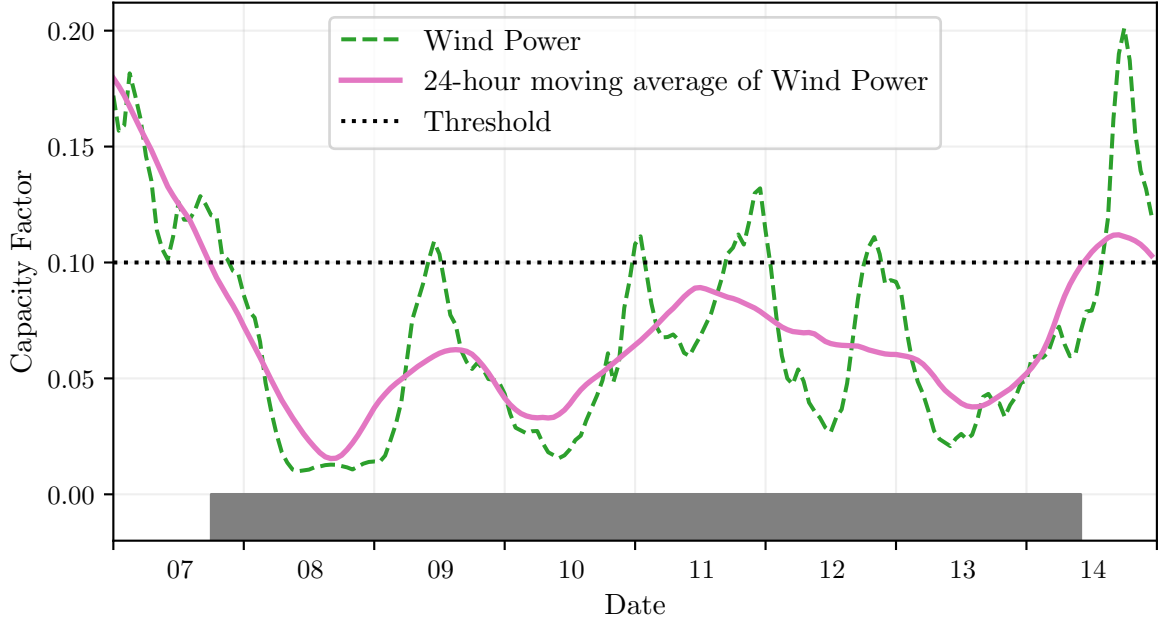


Figure 1: Wind time series of CF (green) and its 24-hour moving average (pink) from the 7th to the 15th of July 2021. The black dashed line indicates the CF threshold. The grey bar shows the period identified as a wind drought under our definition

205 4.1.1. Wind Energy

206 The C3S-E datasets use the Vestas V136/3450 wind turbine power curve,
 207 (Fig. 2a). The Atlite model allows the user to specify the power curve.
 208 We considered the 121 power curves available for download from Renew-
 209 ables.ninja Staffell and Pfenninger (2016). For each power curve, Renew-
 210 ables.ninja also provides four associated smoothed power curves. The smooth-
 211 ing is done using a Gaussian filter with different standard deviations that
 212 depend on the wind speed. A separate wind CF time series for Ireland was
 213 generated for each of the wind turbine power curves and smoothing levels.
 214 The performance of each CF time series was then assessed based on four
 215 skill scores: correlation coefficient (CC), root mean square error (RMSE),
 216 mean bias error (MBE), and area under the curve. The area under the curve
 217 was calculated from histograms of the hourly CF values for the most recent
 218 decade, 2014-2023. Based on these metrics, the most representative power
 219 curve for Ireland was the Enercon E112.4500 power curve with the $0.3w$
 220 smoothing filter.

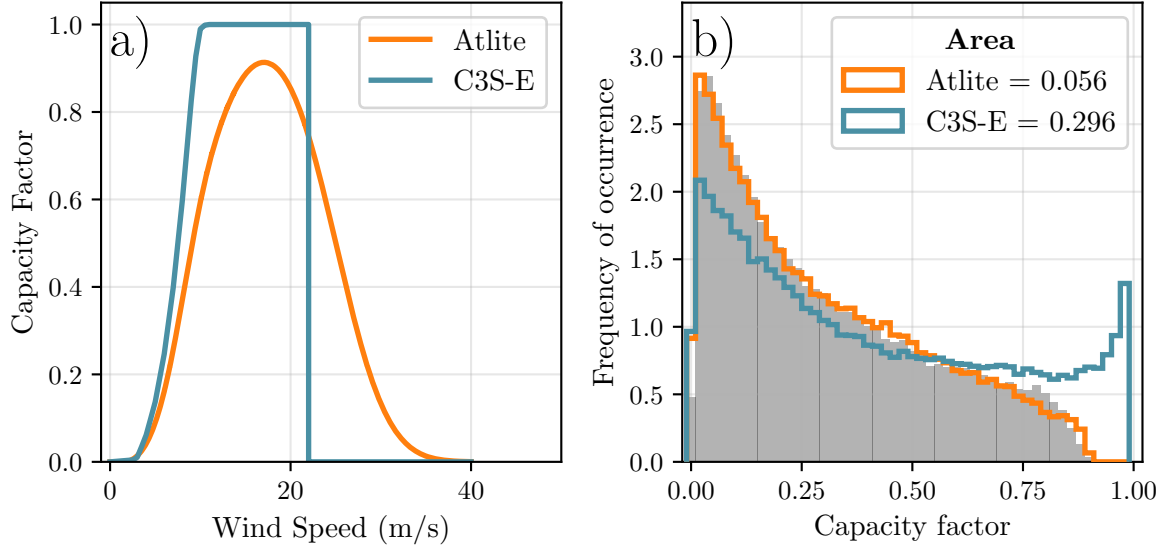


Figure 2: a) Power curves of the Enercon E112.4500 with a 0.3 smoothing filter used by Atlite (orange) and the Vestas V136/3450 used by C3S-E (teal) b) Histograms of wind CF for Ireland from Atlite (orange), C3S-E (teal) and Observed (shaded)

221 The smoothing of the wind turbine power curve represents losses associ-
 222 ated with each turbine, as well as losses such as wake effects between turbines,
 223 which are important when modelling wind energy on larger spatial scales.
 224 The histogram in Fig. 2b shows that the C3S-E power curve tends to under-
 225 estimate low CF values and overestimate higher ones, whereas the smoothed
 226 Atlite power curve more closely follows the recorded wind availability data
 227 from EirGrid.

228 The effect of the difference between the power curves is also visible in
 229 Fig. 3, which shows a density plot of wind CF values. The two C3S-E datasets
 230 are shown to overestimate the observed CF, whereas the Atlite model is in
 231 good agreement with the observed data. The skill scores presented in Table 2
 232 show that Atlite performs better than the C3S-E datasets for all of the skill
 233 scores.

234 Fig. 4 presents the average annual number of wind drought events during
 235 the 2014 to 2023 validation period. The figure presents that Atlite shows
 236 the best agreement overall with the observed frequency and duration of wind
 237 drought events. This pattern is particularly evident for shorter-duration
 238 events, which are the most frequent.

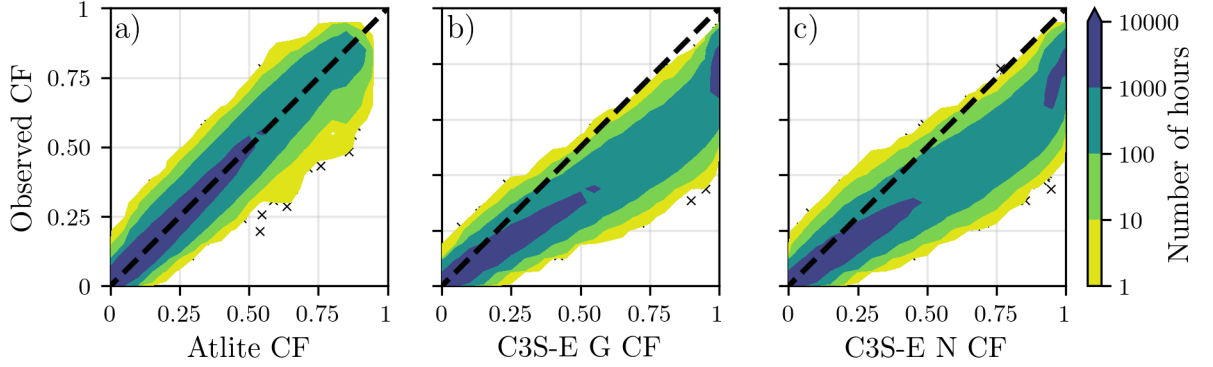


Figure 3: Wind CF density plot of the observed CF (vertical axes) and modelled (horizontal axes) CF data for the a) Atlite, b) C3S-E G and c) C3S-E N models

	Atlite	C3S-E G	C3S-E N
CC	0.981	0.972	0.970
RMSE	0.045	0.177	0.162
MBE	-0.003	0.137	0.121

Table 2: Skill scores for wind power for the three datasets compared to observed data

4.1.2. PV Energy

The Atlite model allows the user to select certain PV panel characteristics. In this study, the three PV panel types available in the Atlite model were considered (CSi, CdTe, Kaneka). Following the same methodology as in the previous section, the three available models were compared using four skill scores (CC, RMSE, MB, and area under the curve). Based on the best-performing metrics, the Breyer PV panel model was selected Beyer et al. (2004), using the Kaneka Hybrid panel option. For all PV farm locations, the azimuth angle is fixed at 180°(due south), and the optimal tilt angle option is applied.

The PV installed capacity available on the spreadsheets from EirGrid represents the Maximum Export Capacity (MEC) and does not accurately reflect the installed PV capacity. To enable actual PV generation potential to be modelled correctly, installed capacities were set at 1.4 times the MEC values. This scaling factor was estimated by analysing proprietary data from individual PV farms provided by EirGrid, which showed that the installed capacities of many farms exceed their MEC values by approximately 40%.

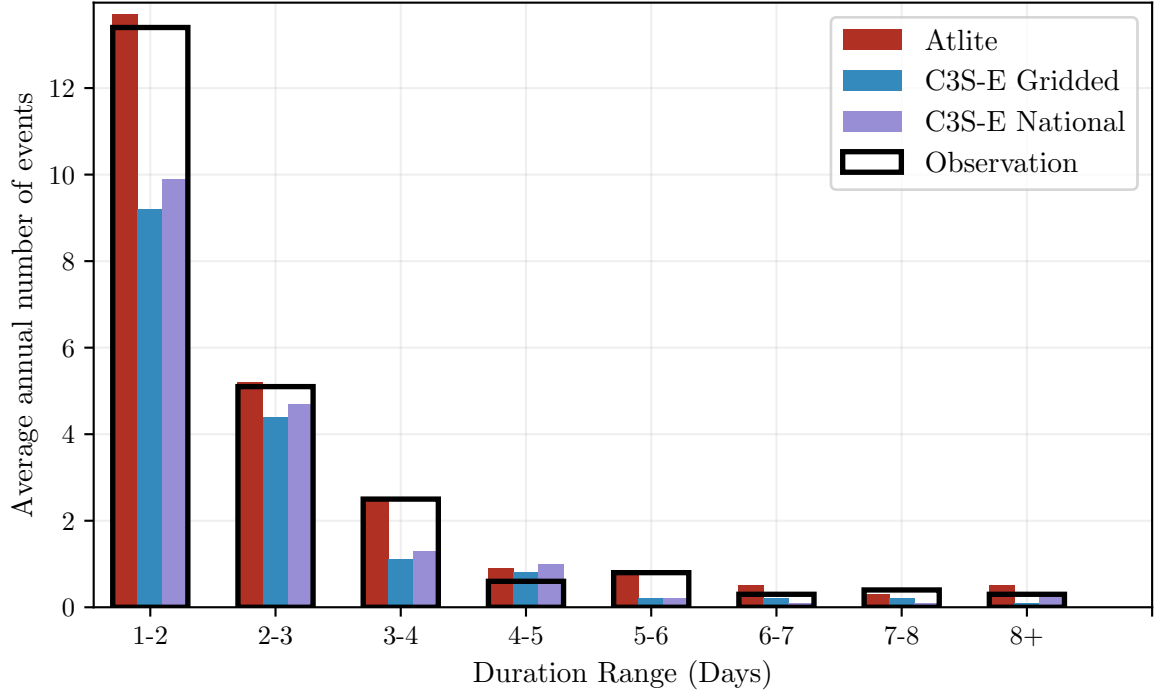


Figure 4: Average annual number of wind drought events for Atlite (red), C3S-E G (blue), C3S-E N (purple), and the observed data (black outline). The wind droughts are identified from 2014 to 2023

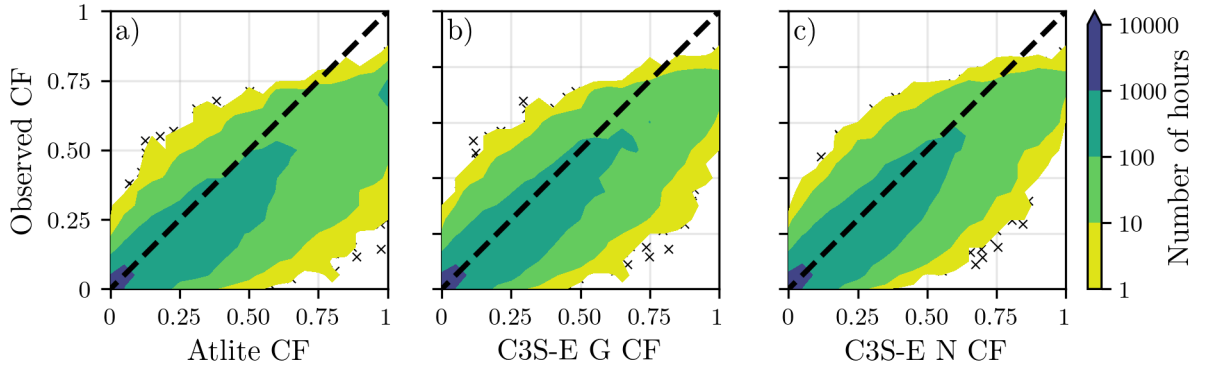


Figure 5: PV CF density plot of the observed (vertical axes) and modelled (horizontal axes) CF series for the a) Atlite, b) C3S-E G and c) C3S-E N models

Figure 5 shows that the three datasets have a similar tendency to overestimate the CF compared to the observed values, especially for high CF values. The skill scores presented in Table 3 indicate that C3S-E G performs best overall, with the lowest RMSE and a high correlation coefficient, suggesting a closer match to observed data. All models show a slight positive bias, with Atlite exhibiting a slightly lower correlation and higher RMSE.

	Atlite	C3S-E G	C3S-E N
CC	0.921	0.931	0.931
RMSE	0.119	0.090	0.113
MBE	0.046	0.027	0.021

Table 3: Skill scores for PV CF for the three datasets compared to observed data

Fig. 6 shows the number of PV drought events during the 2023 validation period across different duration ranges. The figure reveals partial agreement between the three datasets and the observed data, with consistent results noticed for duration ranges of 1-2, 3-4, 7-8, and 8+ days. However, discrepancies appear in the other ranges, where the models diverge from the observed data. The main challenge in validating PV data stems from the recent installation of a large share of Ireland’s PV capacity, leading to uncertainties in PV generation data and the actual generating capacity in the first few months after each farm is connected. With over 65% of the total PV capacity installed in 2023, these data uncertainties significantly impact the ability to perform rigorous validation for PV drought events.

Nevertheless, the goal of this analysis is to assess the combination of wind and PV generation, where the complementary nature of these energy sources mitigates the limitations seen in PV-only results.

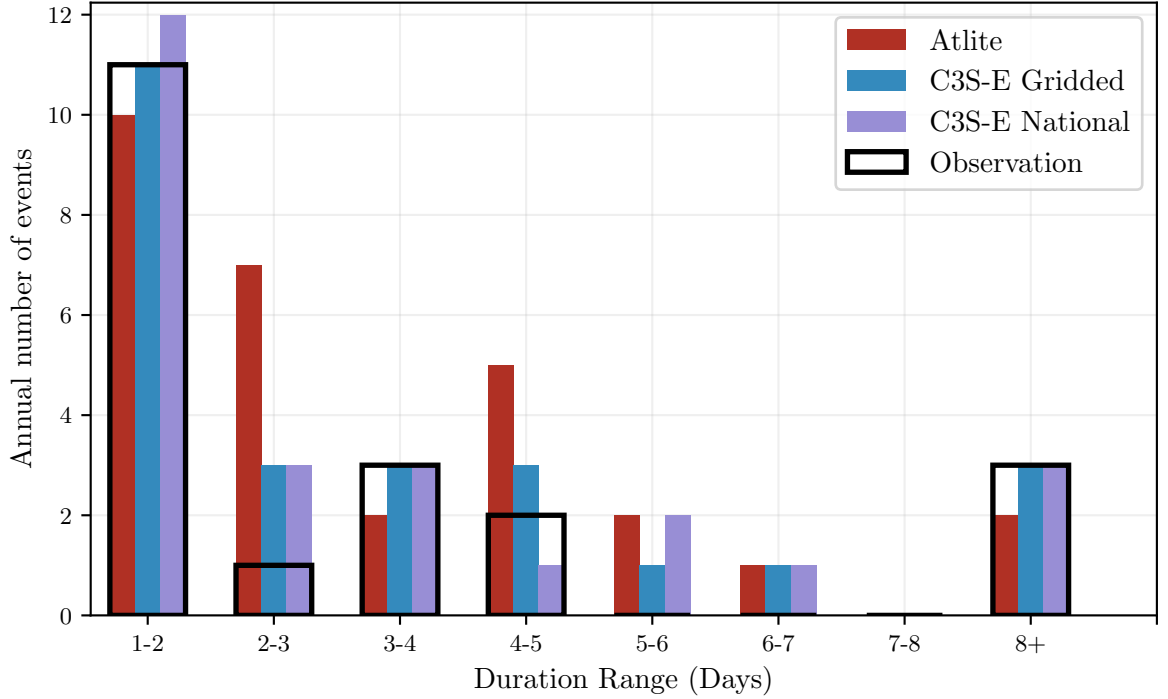


Figure 6: Number of PV drought events for Atlite (red), C3S-E G (blue), and C3S-E N (purple) and the observed data (black outline). The PV droughts are identified for 2023, considering the actual capacity of the system at any given time

276 4.2. Analysis

277 In this section, RES drought events are evaluated under two different
 278 scenarios with fixed installed capacities: the 91W-9PV scenario, with 5.9 GW
 279 of wind capacity and 0.6 GW of PV capacity, and the 57W-43PV scenario,
 280 where wind capacity comprises 11.45 GW and PV capacity increases to 8.6
 281 GW. Both scenarios were driven by 45 years of ERA5 data. Using the RES
 282 drought identification process described in Section 3.5, wind and PV droughts
 283 are first analysed separately before presenting the results for combined (wind
 284 + PV) RES droughts under both scenarios.

285 4.2.1. Annual Number of RES Droughts

286 The first part of the analysis examines the annual number of RES drought
 287 events across the three datasets. For Fig. 7a, the number of events decreases
 288 as the duration range increases, with very few events lasting more than seven

289 days. For Fig. 7b, the number of events also declines as the duration range
 290 extends from one to eight days, followed by a slight increase for longer dura-
 291 tions. This increase is due to extended low-generation periods occurring from
 292 November to March, depending on the dataset. When comparing wind and
 293 PV results (Fig. 7a & b), the median, first, and third quartiles for PV are
 294 consistently higher than or equal to those for wind, across all duration ranges
 295 and datasets. This is due to the typically lower CF of PV power compared
 296 to wind power, especially in a region such as Ireland where solar potential
 297 is limited. PV generation is also zero at night and constrained by the daily
 298 solar cycle, leading to a naturally higher frequency of RES droughts in PV
 299 compared to wind.

300 Fig. 7a & b show the combination of wind and PV under the two capacity
 301 scenarios. In the 91W-9PV scenario (Fig. 7c), the identified RES droughts
 302 closely match those for wind alone, which is expected due to the dominance
 303 of installed wind capacity. In contrast, the 57W-43PV scenario (Fig. 7d)
 304 shows a clear reduction in the number of drought events across all datasets
 305 and durations, with a decrease of the total number of events of 56% for Atlite,
 306 52% for C3S-E G, and 50% for C3S-E N. This reduction is attributed to the
 307 anti-correlation between wind and PV generation.

308 The median, first, and third quartiles for the Atlite dataset are consis-
 309 tently greater than or equal to those of the other two datasets, regardless of
 310 the duration range or type of renewable energy considered. This difference
 311 arises from the wind turbine power curve model used in the C3S-E datasets,
 312 which tends to overestimate the wind CF (Fig. 3). As a result, the overall
 313 number of RES droughts is underestimated in the C3S-E datasets compared
 314 to Atlite.

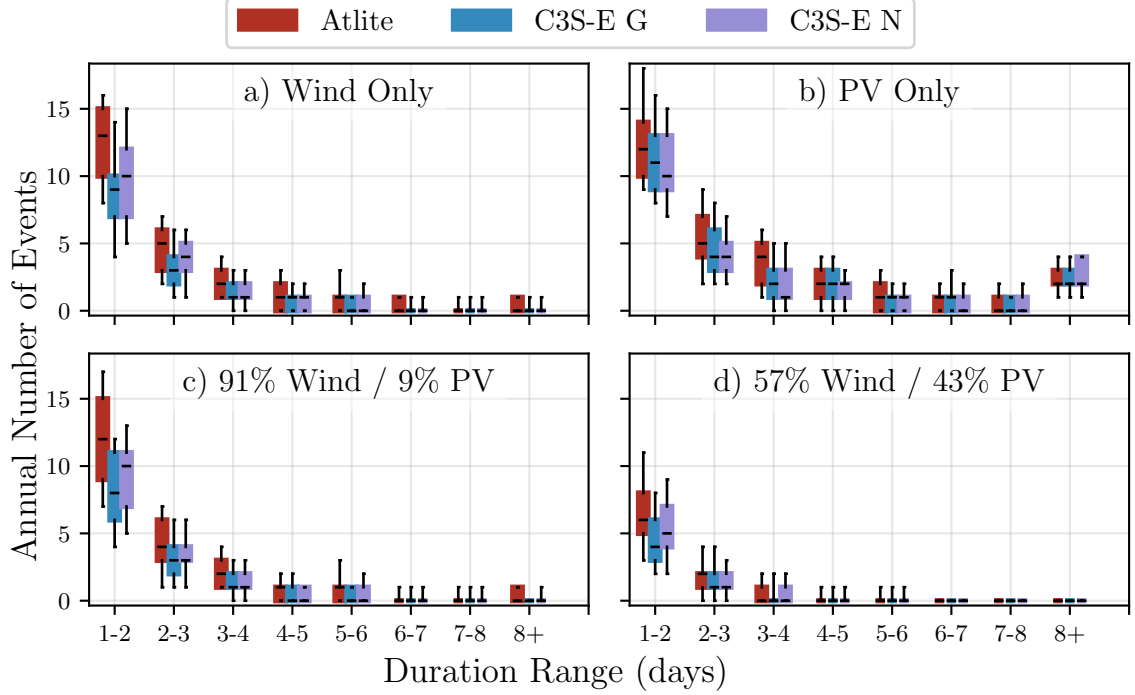


Figure 7: Annual number of RES droughts (from 1979 to 2023) for a) Wind, b) PV, and the combination for the c) 91W-9PV and d) 57W-43PV scenario for Atlite (red), C3S-E G (blue), and C3S-E N (purple). The x-axis represents duration ranges in days (lower bound included), while the y-axis indicates the annual number of events. The boxes display the first and third quartiles and the median is marked by a black line. The whiskers indicate the 5th and 95th percentiles

315 4.2.2. Return Periods of RES Drought Duration

316 The RES drought events identified over the 45-year period were used to
 317 calculate the return periods for different RES drought durations. A return
 318 period refers to the estimated expected interval between occurrences of events
 319 with a specified duration or intensity. Fig. 8 illustrates the return periods
 320 for varying RES drought durations, highlighting how often different drought
 321 lengths are likely to occur across the datasets. This analysis provides insight
 322 into the frequency and likelihood of prolonged low-generation periods, which
 323 is crucial for evaluating the potential impact of RES droughts on energy
 324 reliability and security of supply.

325 For wind (Fig. 8a), the duration of RES droughts increases in a log-

linear fashion across the three datasets. The log-linear trend indicates a predictable relationship between drought duration and occurrence, with longer RES droughts becoming exponentially less likely as duration increases.

For PV (Fig. 8b), Atlite behaves differently than the two C3S-E datasets. The Atlite results show a log-linear increase but reach higher values in general with the longest event lasting forty days. For C3S-E G and C3S-E N, the duration of RES droughts increases in a log-linear pattern for events lasting less than 16 days. Beyond this duration, there is a sharp rise in drought duration for events up to a one-year return period. This sudden increase reflects the impact of winter on PV generation in Ireland, as PV output often remains below the CF threshold for extended periods during winter months. The difference between Atlite and the C3S-E results arises from differences in the datasets near the threshold of 0.1 CF. Atlite remains slightly above the threshold more frequently during these conditions, leading to shorter, more fragmented drought events. In contrast, C3S-E G and C3S-E N tend to fall below the threshold in similar conditions, resulting in longer continuous drought periods, especially during winter. This sensitivity to the threshold highlights how slight model differences can have substantial effects on drought duration estimates, particularly for PV in low-generation conditions.

For the 91W-9PV scenario (Fig. 8c), the return periods mirror those of Fig. 8a, due to the low levels of installed PV capacity. In the 57W-43PV scenario (Fig. 8d), the return periods for RES droughts increase across all durations. For example, the return period for a five-day drought event, shown by the vertical dashed lines in Fig. 8, extends from roughly six months for the 91W-9PV scenario, to four years for the 57W-43PV scenario in the Atlite dataset, and from about fifteen months to around five years in the two C3S-E datasets.

Across Fig. 8a, c, and, d, the return periods in the Atlite dataset are consistently higher than those in the two C3S-E datasets. For instance, in the 91W-9PV scenario (Fig. 8c), an event with a one-year return period lasts six days in the Atlite dataset, compared to only five days in the C3S-E datasets. This difference underscores the importance of model selection when quantifying RES droughts, as each model’s assumptions and parametrisations significantly influence drought duration estimates. Additionally, in all four graphs, the similarity between results from the two C3S-E datasets suggests that assumptions in the Atlite model—such as wind turbine power curve selection and PV panel specifications—have a greater impact on RES drought duration estimates than the precise geographic distribution of RES farms

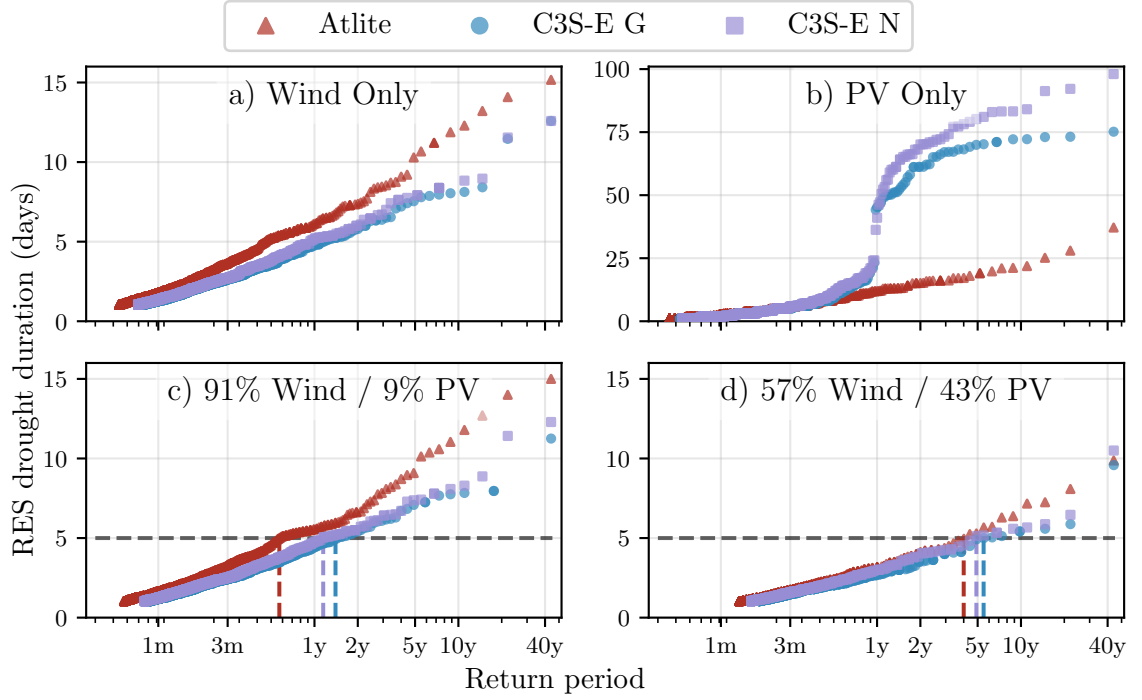


Figure 8: Return periods of the duration of RES droughts (from 1979 to 2023) for a) Wind, b) PV, and the combination for the c) 91W-9PV and d) 57W-43PV scenario, for Atlite (red triangle), C3S-E G (blue circle), and C3S-E N (purple square). The x-axis represents the return period time in a log-scale and the y-axis indicates the duration of RES drought associated with it. The horizontal dashed line marks the 5-day return period, with coloured vertical dashed marking its return period for each dataset

364 when studying the return periods of RES droughts.

365 4.2.3. Seasonal Distribution of RES Droughts

366 The seasonality of RES droughts was analysed by comparing the percent-
367 age of hours in each month classified as part of a RES drought.

368 For Fig. 9a, RES drought percentages are higher in summer than in win-
369 ter. In the Atlite dataset, for instance, an average of 24% of hours in summer
370 (June-July-August) are identified as RES droughts, compared to only 4% in
371 winter (December-January-February). This seasonal variation is influenced
372 by the wind power curve model used to estimate CF, where the shape of the
373 curve in lower wind speed regions (3-10 m/s) leads to significant differences
374 in CF under low wind conditions. In contrast, the results for Fig. 9b show
375 a higher percentage in winter, with RES droughts occurring over 60% of the
376 time regardless of the dataset. The Atlite results show a higher percent-
377 age of RES drought hours for wind, and a slightly lower percentage for PV,
378 compared to the two C3S-E datasets.

379 Similar to previous results, the 91W-9PV scenario (Fig. 9c) shows pat-
380 terns comparable to 9a. However, in the 91W/9PV scenario, the number of
381 hours classified as RES droughts in summer decreases slightly compared to
382 the wind-only scenario. This reduction can be explained by the contribution
383 of PV generation during the summer months in the 91W-9PV scenario, even
384 though it constitutes only 11% of total capacity. Since the number of RES
385 drought hours for PV in summer is near zero, this small contribution has a
386 noticeable impact on reducing overall drought hours. In the 57W-43PV sce-
387 nario (Fig. 9d), all three datasets show a reduction in monthly RES drought
388 frequency. Annual reductions in median RES drought frequency are observed
389 across the datasets, dropping from 14% to 5% for Atlite, from 8% to 3% for
390 C3S-E G, and from 9% to 4% for C3S-E N. The balanced mix of wind and
391 PV power in this scenario reduces the seasonal signal overall and significantly
392 decreases the percentage of RES drought hours in the summer.

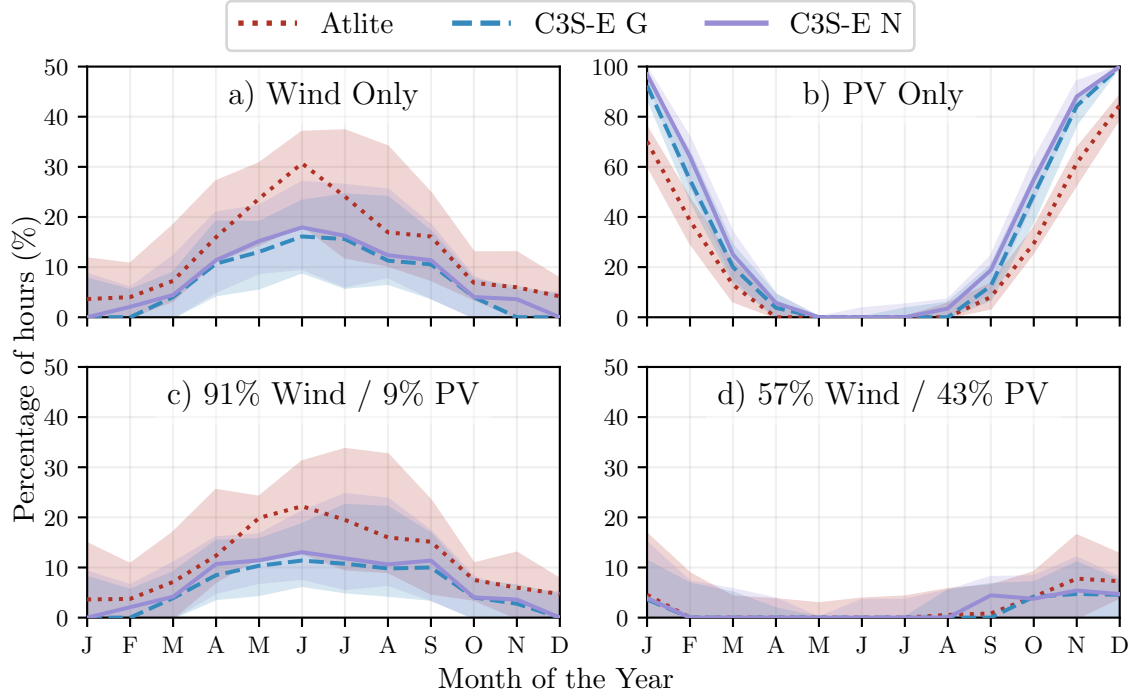


Figure 9: Percentage of hours in a month which are part of a RES drought (from 1979 to 2023) for a) Wind, b) PV, and the combination for the c) 91W-9PV and d) 57W-43PV scenario, for Atlite (red dotted), C3S-E G (blue dashed), and C3S-E N (purple solid). The x-axis represents the month of the year, and the y-axis indicates the percentage of hours. Lines correspond to the median values and the area between the first and third quartiles is shaded.

5. Discussion and Conclusions

This study has investigated the ability of three RES models to represent RES droughts: Atlite, C3S-E G, and C3S-E N. One of the most evident differences is how each dataset incorporates the specific locations of RES farms. Both Atlite and C3S-E G consider the locations of wind and PV farms, which should, in theory, provide a more accurate representation of RES generation. While this approach slightly improves PV models, our analysis indicates that for wind energy, the Atlite dataset performs better overall, especially in its close alignment with observed data for wind generation estimates. This finding suggests that, although the inclusion of RES farm locations is beneficial, the accuracy of the RES model is more strongly influenced by underlying

404 model assumptions, such as selecting an appropriate wind power curve.

405 Atlite shows the best alignment with observed data for wind generation.
406 Differences between the models are smaller for PV, with C3S-G performing
407 marginally better than the other two. The results show that the two C3S-
408 E datasets (C3S-E G and C3S-E N) consistently yield similar outcomes,
409 indicating that their methodological differences have minimal impact. This
410 distinction was also evident in the analysis, where Atlite reported higher
411 return periods and a greater number of RES droughts, especially in scenarios
412 with a balanced share of RES. Again, the results from RES drought modelling
413 rely more on the precision of the wind power curve and PV panel models
414 than on the specific locations of RES farms. Atlite’s superior performance
415 highlights the importance of selecting validated models for assessing RES
416 drought risks. This careful model selection can better quantify risks, support
417 effective planning, and avoid the potential underestimation of capacity needs,
418 which is essential for ensuring energy security.

419 Looking at the 57W-43PV scenario, the analysis showed a significant im-
420 provement in the management of RES droughts due to the complementary
421 nature of wind and PV generation. Wind and PV together perform better
422 in terms of reducing drought frequency and duration than either would in-
423 dividually, largely because of the seasonal anti-correlation between the two
424 energy sources. This diversification reduces the seasonal impact on RES
425 droughts, as PV generation peaks in the summer and wind generation is
426 more consistent in winter. Ireland currently has a highly wind-dependent
427 energy system, but with ambitious targets for PV installations in the coming
428 years, the energy mix is expected to approach a balance between wind and
429 PV capacity. While this balanced approach offers a more stable and secure
430 energy supply by mitigating RES drought risks, it is important to note that
431 having similar wind and PV capacities may not optimise other aspects, such
432 as annual energy production or meeting nighttime loads. For policymakers,
433 these findings underscore the importance of meeting these capacity targets
434 to enhance energy security through diversification. Additionally, the choice
435 of model for RES drought assessment becomes increasingly critical as more
436 renewable capacity is integrated into the system.

437 Future work is planned to extend the current analysis. First, climate pro-
438 jection data will be integrated with different energy scenarios, incorporating
439 the addition of offshore wind, to better understand how climate change might
440 affect RES droughts. Second, expanding the geographic domain of the study
441 to include the EU would provide a more comprehensive understanding of

RES droughts in an interconnected energy grid. This would require extensive verification across all EU countries, making it a more complex but highly relevant challenge.

References

- Ali Khan Niazi, K., Victoria, M., 2023. Comparative analysis of photovoltaic configurations for agrivoltaic systems in europe. *Progress in Photovoltaics: Research and Applications* 31, 1101–1113.
- Allen, S., Otero, N., 2023. Standardised indices to monitor energy droughts. *Renewable Energy* 217, 119206. doi:10.1016/j.renene.2023.119206.
- Beyer, H.G., Heilscher, G., Bofinger, S., 2004. A robust model for the mpp performance of different types of pv-modules applied for the performance check of grid connected systems. *Eurosun* , 8.
- Bloomfield, H.C., Brayshaw, D.J., Shaffrey, L.C., Coker, P.J., Thornton, H.E., 2016. Quantifying the increasing sensitivity of power systems to climate variability. *Environmental Research Letters* 11, 124025.
- Bloomfield, H.C., Brayshaw, D.J., Troccoli, A., Goodess, C.M., De Felice, M., Dubus, L., Bett, P.E., Saint-Drenan, Y.M., 2021. Quantifying the sensitivity of european power systems to energy scenarios and climate change projections. *Renewable Energy* 164, 1062–1075. doi:10.1016/j.renene.2020.09.125.
- Bracken, C., Voisin, N., Burleyson, C.D., Campbell, A.M., Hou, Z.J., Broman, D., 2024. Standardized benchmark of historical compound wind and solar energy droughts across the Continental United States. *Renewable Energy* 220, 119550. doi:https://doi.org/10.1016/j.renene.2023.119550.
- Brown, P.T., Farnham, D.J., Caldeira, K., 2021. Meteorology and climatology of historical weekly wind and solar power resource droughts over western North America in ERA5. *SN Applied Sciences* 3, 814. doi:10.1007/s42452-021-04794-z.
- (C3S), C.C.C.S., 2020. Climate and energy indicators for Europe from 1979 to present derived from reanalysis. doi:10.24381/cds.4bd77450. accessed on 28-11-2024.

473 Dubus, L., Saint-Drenan, Y., Troccoli, A., De Felice, M., Moreau, Y., Ho-
 474 Tran, L., Goodess, C., Amaro E Silva, R., Sanger, L., 2023. C3S Energy: A
 475 climate service for the provision of power supply and demand indicators for
 476 Europe based on the ERA5 reanalysis and ENTSO-E data. *Meteorological*
 477 *Applications* 30, e2145. doi:10.1002/met.2145.

478 EuroStat, 2023. Renewable Energy Statistics.

479 Gangopadhyay, A., Seshadri, A.K., Sparks, N.J., Toumi, R., 2022. The
 480 role of wind-solar hybrid plants in mitigating renewable energy-droughts.
 481 *Renewable Energy* 194, 926–937. doi:10.1016/j.renene.2022.05.122.

482 Hersbach, H., Bell, B., Berrisford, P., Hirahara, S., Horányi, A., Muñoz-
 483 Sabater, J., Nicolas, J., Peubey, C., Radu, R., Schepers, D., et al., 2020.
 484 The ERA5 global reanalysis. *Quarterly Journal of the Royal Meteorological*
 485 *Society* 146, 1999–2049. doi:10.1002/qj.3803.

486 Hofmann, F., Hampp, J., Neumann, F., Brown, T., Hörsch, J., 2021. Atlite:
 487 a lightweight Python package for calculating renewable power potentials
 488 and time series. *Journal of Open Source Software* 6, 3294.

489 of Ireland, G., 2023. Climate Action Plan 2024. 3.

490 Ireland, S.E.A., 2024. National Energy Projections 2024.

491 Kapica, J., Jurasz, J., Canales, F.A., Bloomfield, H., Guezgouz, M., De Fe-
 492 lice, M., Kobus, Z., 2024. The potential impact of climate change on
 493 european renewable energy droughts. *Renewable and Sustainable Energy*
 494 *Reviews* 189, 114011. doi:10.1016/j.rser.2023.114011.

495 Kaspar, F., Borsche, M., Pfeifroth, U., Trentmann, J., Drücke, J., Becker,
 496 P., 2019. A climatological assessment of balancing effects and shortfall
 497 risks of photovoltaics and wind energy in germany and europe. *Advances*
 498 *in Science and Research* 16, 119–128. doi:10.5194/asr-16-119-2019.

499 Li, J., Zhao, Z., Xu, D., Li, P., Liu, Y., Mahmud, M.A., Chen, D., 2023. The
 500 potential assessment of pump hydro energy storage to reduce renewable
 501 curtailment and co2 emissions in northwest china. *Renewable Energy* 212,
 502 82–96.

503 Mayer, M.J., Biró, B., Szücs, B., Aszódi, A., 2023. Probabilis-
504 tic modeling of future electricity systems with high renewable energy
505 penetration using machine learning. *Applied Energy* 336, 120801.
506 doi:10.1016/j.apenergy.2023.120801.

507 Mockert, F., Grams, C.M., Brown, T., Neumann, F., 2023. Meteorological
508 conditions during periods of low wind speed and insolation in Germany:
509 The role of weather regimes. *Meteorological Applications* 30, e2141.

510 Ohba, M., Kanno, Y., Nohara, D., 2022. Climatology of dark doldrums
511 in japan. *Renewable and Sustainable Energy Reviews* 155, 111927.
512 doi:10.1016/j.rser.2021.111927.

513 Otero, N., Martius, O., Allen, S., Bloomfield, H., Schaeffli, B., 2022. Char-
514 acterizing renewable energy compound events across Europe using a lo-
515 gistic regression-based approach. *Meteorological Applications* 29, e2089.
516 doi:10.1002/met.2089. 13.

517 Parzen, M., Abdel-Khalek, H., Fedotova, E., Mahmood, M., Frysztacki,
518 M.M., Hampp, J., Franken, L., Schumm, L., Neumann, F., Poli, D., et al.,
519 2023. Pypsa-earth. a new global open energy system optimization model
520 demonstrated in africa. *Applied Energy* 341, 121096.

521 Raynaud, D., Hingray, B., François, B., Creutin, J., 2018. Energy droughts
522 from variable renewable energy sources in European climates. *Renewable*
523 *Energy* 125, 578–589. doi:https://doi.org/10.1016/j.renene.2018.02.130.

524 Rinaldi, K.Z., Dowling, J.A., Ruggles, T.H., Caldeira, K., Lewis, N.S.,
525 2021. Wind and Solar Resource Droughts in California Highlight the
526 Benefits of Long-Term Storage and Integration with the Western In-
527 terconnect. *Environmental Science and Technology* 55, 6214–6226.
528 doi:10.1021/acs.est.0c07848.

529 Saint-Drenan, Y.M., Wald, L., Ranchin, T., Dubus, L., Troccoli, A., 2018.
530 An approach for the estimation of the aggregated photovoltaic power gen-
531 erated in several European countries from meteorological data. *Advances*
532 *in Science and Research* 15, 51–62. doi:10.5194/asr-15-51-2018.

533 SONI, E., . System and Renewable Data Reports.

- 534 Staffell, I., Pfenninger, S., 2016. Using bias-corrected reanalysis to sim-
535 ulate current and future wind power output. *Energy* 114, 1224–1239.
536 doi:10.1016/j.energy.2016.08.068.
- 537 van der Wiel, K., Stoop, L.P., Van Zuijlen, B.R.H., Blackport, R., Van den
538 Broek, M.A., Selten, F.M., 2019. Meteorological conditions leading to
539 extreme low variable renewable energy production and extreme high en-
540 ergy shortfall. *Renewable and Sustainable Energy Reviews* 111, 261–275.
541 doi:10.1016/j.rser.2019.04.065.